

Article

Approximation of Stochastic Quasi-Periodic Responses of Limit Cycles in Non-Equilibrium Systems under Periodic Excitations and Weak Fluctuations

Kongming Guo ¹, Jun Jiang ^{2,*} and Yalan Xu ¹

¹ Research Center of Applied Mechanics, School of Mechano-Electronic Engineering, Xidian University, Xi'an 710071, China; kmguo@xidian.edu.cn (K.G.); ylxu@mail.xidian.edu.cn (Y.X.)

² State Key Laboratory for Strength and Vibration, Xi'an Jiaotong University, Xi'an 710049, China

* Correspondence: jun.jiang@mail.xjtu.edu.cn; Tel.: +86-029-8266-8754

Received: 17 May 2017; Accepted: 14 June 2017; Published: 15 June 2017

Abstract: A semi-analytical method is proposed to calculate stochastic quasi-periodic responses of limit cycles in non-equilibrium dynamical systems excited by periodic forces and weak random fluctuations, approximately. First, a kind of $1/N$ -stroboscopic map is introduced to discretize the quasi-periodic torus into closed curves, which are then approximated by periodic points. Using a stochastic sensitivity function of discrete time systems, the transverse dispersion of these circles can be quantified. Furthermore, combined with the longitudinal distribution of the circles, the probability density function of these closed curves in stroboscopic sections can be determined. The validity of this approach is shown through a van der Pol oscillator and Brusselator.

Keywords: weak fluctuation; non-equilibrium system; quasi-periodic; stochastic sensitivity function; probability density function

1. Introduction

Random fluctuation (also called noise) is inevitable in dynamical systems. Due to the interactions between nonlinearity and stochasticity, in nonlinear dynamical systems many phenomena with new regimes can be induced by even weak fluctuations. For the systems far from equilibrium, fluctuation plays an important role in self-organization induced order phenomena [1]. The various fluctuation-induced behaviors, like stochastic resonance [2,3], noise-induced synchronization [4], coherence resonance [5], noise-induced chaos [6], fluctuation-induced escape [7], and noise-induced bifurcation [8] have attracted the attention of a large number of researchers from various fields as central problems in modern nonlinear dynamics theories.

The stationary state, which is called an attractor in nonlinear dynamical system theory, plays the central role in the analysis of the nonlinear systems. Fluctuation can drive the trajectory of the attractor, leave it, and form a "blurred" state around it (Figure 1). This state is named a stochastic attractor [9], which is one kind of almost invariant sets in mathematical language [10]. When multi-stable systems are disturbed by additive Gaussian white noise, all deterministic attractors become metastable stochastic attractors. Thereby, the responses of the disturbed systems can be seen as combinations of stochastic attractors and hopping between them. When noise is weak, the lifetime of metastable states is very long, although this metastable state will finally escape to other metastable states. Thus, if we choose initial conditions in the vicinity of the deterministic attractor, a very long transient probability density distribution will form that can be considered as a steady state probability density distribution for a finite observation time (Figure 2). Thus, picking initial conditions in the vicinity of the underlying deterministic attractor, the probability density function (PDF) of

stochastic attractor can be computed by a Monte Carlo simulation. Monte Carlo simulations are very time consuming, analytical methods that are still indispensable. For differential dynamical systems, the Fokker-Planck equation (FPE) [11] gives the most detailed description of PDF evolution, but it is difficult to get close-form solutions of FPE for systems without detailed balance except for some special systems [12]. Thus, until now, many approximate methods have been raised to solve FPE under various specific circumstances, such as the stochastic average method [13], path-integral method [14], finite element method [15], Galerkin-Ulam-like method [16], cell-mapping method [8], etc. Most of these methods are proposed to solve the response of systems with weak nonlinearities. For stronger nonlinear systems, they cannot work well.

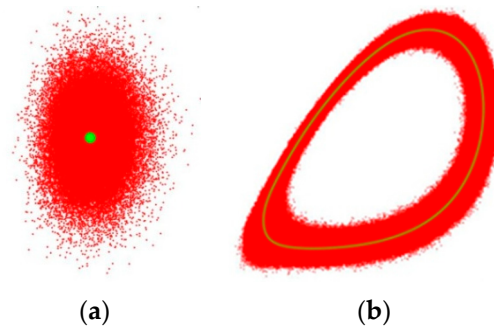


Figure 1. (a) Deterministic (green) and stochastic stationary point attractor (red); and (b) deterministic (green) and stochastic closed curve attractor (red).

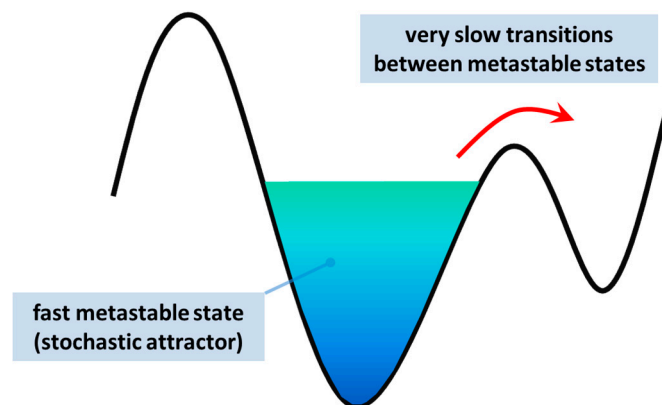


Figure 2. A stochastic attractor as a metastable state when fluctuation is weak and the average first passage time to another metastable state is very large. Thus, the probability density function of the stochastic attractor can be considered as steady-state for a finite observation time.

Based on quasi-potential (also called pseudo-potential) theory [17–19], Bashkirtseva [20] proposed the stochastic sensitivity function (SSF) method to describe the transverse dispersion of stochastic attractors. In this method, distribution of stochastic attractor is expressed by confidence ellipse or confidence band around the deterministic attractor. The original deterministic attractor is calculated numerically so the problem of nonlinearity is evaded. The SSF method provides an idea for the construction of a PDF of weak fluctuation generated stochastic attractors, especially a stochastic periodic attractor [21].

The simplest kind of non-equilibrium stationary state is the limit cycle attractor (see Figure 3). Based on the understanding that weak additive noise cannot change the probability distribution along the closed curve type attractors, a PDF decomposition method [22] is proposed by the authors to construct an n -dimensional PDF of the stochastic closed-curve attractor using a one-dimensional in-attractor PDF and an $(n - 1)$ -dimensional out-of-attractor PDF. The former is calculated in the

deterministic system numerically and the latter can be quantified by the SSF method. Consequently, the n -dimensional PDF of the stochastic closed-curve attractor can be expressed by production of a one-dimensional in-attractor PDF and an $(n - 1)$ -dimensional out-of-attractor PDF. In the SSF method, only a weak noise condition is required, so it can be used in strongly nonlinear systems.

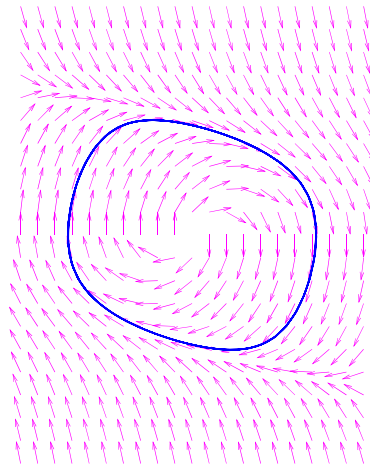


Figure 3. A limit cycle (blue) in a 2D non-equilibrium system. The arrows represent the direction of the vector field in which there is an obvious circulation.

Periodic force is a common kind of excitation which widely exists in various systems. When a limit cycle attractor suffers periodic excitation, the system becomes non-autonomous and the response is quasi-periodic for non-degenerate conditions. In the augmented phase space the quasi-periodic attractor takes the form of an invariant torus. The quasi-periodic attractor is of great significance in many fields, like celestial mechanics, mechanical vibrations, and lasers, etc. While the excitation contains both periodic component and random fluctuation, the quasi-periodic attractor diffuses to a stochastic attractor. Thus, it is of great significance to obtain a PDF of the stochastic quasi-periodic attractor in periodic and random excited non-equilibrium systems. A theoretical investigation of the SSF of the quasi-periodic attractor in autonomous systems is given in [23]. In this paper, for quasi-periodic attractors in non-autonomous systems, a simpler method is used to obtain the SSF based on the SSF of discrete-time systems proposed in [24]. Compared with the works in [24], a kind of $1/N$ -stroboscopic map is used in this paper to discretize the torus of the non-autonomous system into quasi-periodic circles in stroboscopic sections, so that the SSF method for circles in discrete-time systems is extended to tori in non-autonomous systems. Furthermore, not only confidence intervals, but also PDF of the circles in observed stroboscopic sections, can be approximately obtained in this paper using a kind of PDF decomposition method for weak additive noise-disturbed systems.

If the rotation number of the response is rational, the attractor degenerates, becoming periodic. Note that in this situation the method proposed in this paper can also be used. In fact, in order to obtain the SSF of the quasi-periodic circle with an irrational rotation number, the circle is just an approximate with a periodic one with a rational rotation number. Since periodicity can be considered as a special case of quasi-periodicity, the term “quasi-periodic” is used in the title of the paper.

This paper is structured as follows: In Section 2 the PDF decomposition method of closed curve attractors is introduced. Section 3 covers the method to get SSF of stochastic quasi-periodic attractor in non-autonomous systems by the periodic approximation method and $1/N$ -stroboscopic map. In Section 4 the procedure to construct a PDF of a stochastic quasi-periodic attractor in stroboscopic sections is listed. The validity of the proposed method is verified by van der Pol oscillator and Brusselator in Section 5. Conclusions are drawn in the final section.

2. Density Distribution of the Stochastic Attractor

When noise is vanishingly small, the probability of finding the state in the direction “along” an attractor (called in-attractor PDF) is independent of the intensity of the noise and coincides with the deterministic invariant measure. When an attractor suffers additive Gaussian noise, points deviate from it and form a Gaussian distribution in the orthogonal hyperplane. It was found in [22] that, although the Gaussian distributions in different parts of the attractor can intersect each other (Figure 4b), which means hopping between different parts of the attractor and, thus, changing the invariant measure along this attractor, when the noise is weak, due to the Gaussian shape of orthogonal distribution, the intersection only happens in the tails of the Gaussian distributions (Figure 4a) and the hopping between different parts can be considered as a rare event. Thus, it can be considered that weak additive Gaussian noise just drives points away from the deterministic attractor in the transverse direction [17] because the in-attractor probability flux reaches a dynamical balance, and the points of stochastic attractor form a Gaussian distribution around the deterministic attractor in the transverse direction (called out-of-attractor PDF). Note that whether the noise is weak or not depends on the attractors. If the attractor is not sensitive to noise, the “weak” noise can have a relatively larger intensity.

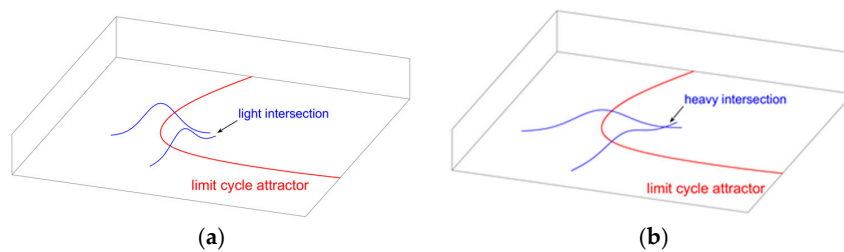


Figure 4. (a) Noise is weak, and the intersection between different parts is light; and (b) noise is not weak, the intersection between different parts is heavy.

Therefore, for the stochastic attractor generated by weak additive Gaussian noise: (1) the in-attractor PDF equals the distribution of the original deterministic attractor; and (2) the out-of-attractor PDF is Gaussian. Based on these understanding, a PDF decomposition method can be used to construct PDF of stochastic attractors. Suppose the dimension of the system and deterministic attractor is n and n_a , respectively. Two kinds of coordinates are needed in this method. One is the global in-attractor n_a -dimensional coordinate presenting the location of point x^* in the deterministic attractor which is nearest to the studied point x , the other is the local $(n - n_a)$ -dimensional out-of-attractor coordinate which is defined in the transverse direction at point x^* (see Figure 5 for planar limit cycle attractors). Thus, the n -dimensional PDF of stochastic attractor can now be decomposed into two independent low-dimensional PDF approximately. One is the n_a -dimensional PDF, ρ_τ , which describes the in-attractor PDF, and the other is the $(n - n_a)$ -dimensional Gaussian form PDF, ρ_n , that represents the out-of-attractor PDF, namely:

$$\rho(x) \approx \rho_\tau(s(x^*))\rho_n(z(x)) \tag{1}$$

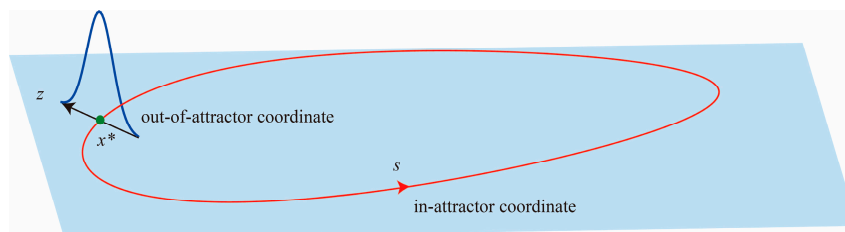


Figure 5. In-attractor coordinate s and out-of-attractor coordinate z at point x^* on a planar limit cycle attractor.

From above discussion, the in-attractor PDF of stochastic attractor can be determined from the deterministic systems, while the out-of-attractor PDF takes the Gaussian form:

$$\rho_n(\mathbf{z}(\mathbf{x})) \approx \frac{1}{(2\pi)^{\frac{n-1}{2}} |\mathbf{M}|^{\frac{1}{2}}} \exp\left\{-\frac{1}{2} \mathbf{z}^T \mathbf{M}^{-1} \mathbf{z}\right\} \quad (2)$$

where \mathbf{M} is $(n - n_a) \times (n - n_a)$ covariance matrix of this Gaussian distribution. In the following section, approaches to obtain matrix \mathbf{M} based on the SSF will be detailed.

3. The SSF of Stochastic Quasi-Periodic Attractor in Non-Autonomous Systems

3.1. 1/N-Period Stroboscopic Map

Consider a continuous-time non-autonomous dynamical system:

$$\dot{\mathbf{x}} = \mathbf{f}(\mathbf{x}, t) \quad (3)$$

where $\mathbf{f}(\mathbf{x}, t)$ is n -dimensional non-autonomous vector field depending on both state vector \mathbf{x} and time t .

For periodic-driven non-autonomous systems (Equation (3)) with period T , the phase of the driving force is introduced as:

$$\theta = 2\pi \frac{t}{T} + \theta_0 \quad \text{mod } 2\pi \quad (4)$$

Considering θ as a new variable, the non-autonomous systems (Equation (3)) can be rewritten as an $(n + 1)$ -dimensional augmented autonomous system:

$$\begin{aligned} \dot{\mathbf{x}} &= \mathbf{f}(\mathbf{x}, \theta) \\ \dot{\theta} &= \frac{2\pi}{T} \end{aligned} \quad (5)$$

Thus, the state of this extended system is determined by \mathbf{x} and θ .

Stroboscopic map is often used to observe the response of system (Equation (5)). Taking snapshots of the trajectory of Equation (5) at discrete phases $\theta_i = i\Delta\theta$ (i is a natural number and $\Delta\theta$ is the sampling phase interval) and registering the state \mathbf{x} at each instant, a series of points $\{\mathbf{x}_i\}$ is generated. Point \mathbf{x}_{i+1} is determined only by the previous point \mathbf{x}_i , thus a discrete map can be defined as:

$$\mathbf{x}_{i+1} = M_{si}(\mathbf{x}_i) \quad (6)$$

which M_{si} is the so-called stroboscopic map. In fact, the points $\{\mathbf{x}_i\}$ are the intersections between the trajectory and the stroboscopic sections, which are defined as:

$$\Sigma_i = \left\{ (\mathbf{x}, t) \in R^n \times S^1 \mid \theta = \theta_0 + i\Delta\theta \right\} \quad (7)$$

where S^1 means a one-dimensional circle space.

Often the sampling phase interval $\Delta\theta$ is chosen to be 2π , and this kind of stroboscopic map will be called a one-period stroboscopic map in this article. There is only one stroboscopic section in a one-period stroboscopic map. In this case, M_{si} is identical in every iteration step i and often lacks an analytical formula. Further, the information of the system in the phase interval $[0, 2\pi]$ is lost. Thus, in order to solve these problems and consider persistent fluctuation along the trajectory, a kind of 1/N-period stroboscopic map is introduced [25].

Note from Equation (4) that if $\Delta\theta \rightarrow 0$, the time interval Δt also tends to zero, the linear approximation of the map (Equation (6)) can be used to estimate the one-step map of Equation (6) from $(\theta_0 + i\Delta\theta)$ to $(\theta_0 + (i + 1)\Delta\theta)$; that is:

$$\mathbf{x}_{i+1} = \exp(J_i \Delta t) \mathbf{x}_i \quad (8)$$

where:

$$J_i = \partial f / \partial x |_{x=x_i, t=t_0+i\Delta t} \tag{9}$$

is the Jacobian matrix of Equation (3) at point x_i and time $t_0 + i\Delta t$. t_0 is the initial time.

Thus, suppose N is a large positive integer, the sampling phase interval of the stroboscopic map can be set to:

$$\Delta\theta = 2\pi/N \tag{10}$$

Consequently, the sampling time interval is:

$$\Delta t = T/N \tag{11}$$

Thus, a new stroboscopic map can be written in the form of Equation (8), approximately. This new map is named the $1/N$ -period stroboscopic map (see Figure 6). Since the phase θ is in S^1 and $\Sigma_i = \Sigma_{i+N}$, there are totally N stroboscopic sections to be considered.

Through this new map, a torus attractor of Equation (3) is discretized into N closed curves $\{\Gamma_1, \dots, \Gamma_N\}$ by N stroboscopic sections $\{\Sigma_1, \dots, \Sigma_N\}$ (see Figure 7).

Now consider the case that Equation (3) suffers additive Gaussian white noise disturbances:

$$\dot{x} = f(x, t) + \varepsilon\sigma\xi(t) \tag{12}$$

where ξ is n -dimensional Gaussian white noise, σ is an $n \times n$ matrix which indicates the disturbed states, and ε is the noise intensity.

The $1/N$ -period stroboscopic map of Equation (12) can be approximately written as:

$$x_{i+1} = \exp(J_i\Delta t)x_i + \varepsilon\sigma\Delta w_i \tag{13}$$

where:

$$\Delta w_i = \sqrt{\Delta t}\xi \tag{14}$$

is the increment of Wiener process within the time interval $[t_0 + i\Delta t, t_0 + (i + 1)\Delta t]$.

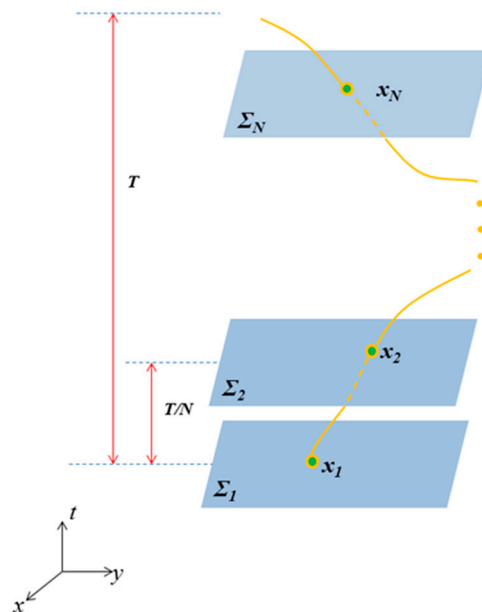


Figure 6. $1/N$ -period stroboscopic map of a two-dimensional non-autonomous system.

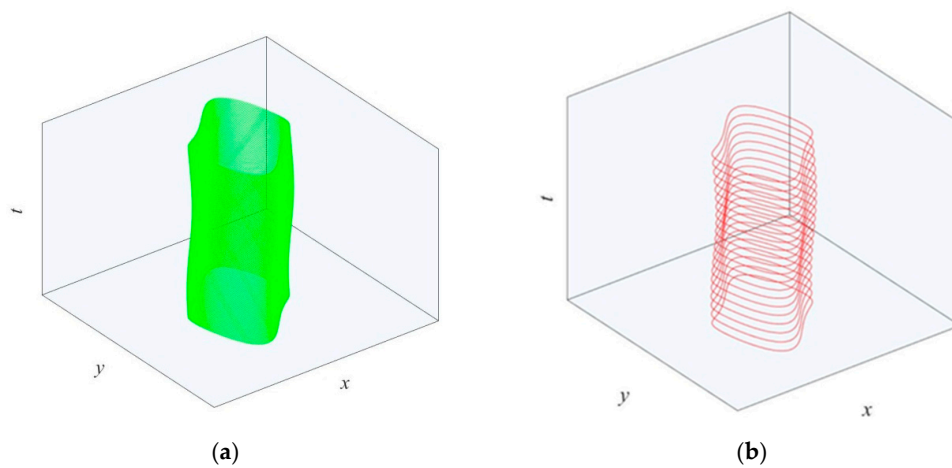


Figure 7. (a) A torus in non-autonomous system; and (b) its corresponding discrete closed curves in stroboscopic sections.

3.2. Periodic Approximation of Quasi-Periodic Attractor

From Section 3.1, the distribution of a stochastic torus can be expressed by distributions of stochastic circles in the stroboscopic sections. Usually the winding number of torus is irrational so the circle in any stroboscopic section is quasi-periodic. If the winding number of the torus is rational, the torus is in resonance and degenerate to periodic solution. The circles in stroboscopic sections also degenerate to periodic points, in which case the circles $\{\Gamma_1, \dots, \Gamma_N\}$ are often called invisible attractors [26]. This kind of degeneration is called resonance or synchronization. In this situation the SSF method in [24] can be used directly and will not be discussed in this section.

The SSF method can be used to obtain the transverse density distribution of circles $\{\Gamma_i\}$ in stroboscopic sections. In order to adapt the SSF method to quasi-periodic circles, periodic approximation is used to approximate the quasi-periodic circle into a periodic one.

A simple method in [9] is utilized to implement this approximation. First, we generate a long series of points $\{x_{\Gamma_i}\}$ along the circle, then find the point x_{Γ_k} which has the minimal distance from the first point x_{Γ_1} . Finally, the quasi-periodic circle is approximated by a resonant one containing periodic- k points on it. Note that the points are periodic- k in a one-period stroboscopic map and, thus, period- kN in a $1/N$ -period stroboscopic map.

If one circle Γ_i in $\{\Gamma_1, \dots, \Gamma_N\}$ has been approximated by a periodic one, this means that all of the closed curves $\{\Gamma_i\}$ are in resonance and the quasi-periodic torus attractor degenerates to periodic.

3.3. Transverse Distribution of the Closed Curves in Stroboscopic Sections

In Section 3.2 the method to approximate quasi-periodic circles by a resonant one is stated. For the quasi-periodic attractor, the torus is exponentially stable and so all circles $\{\Gamma_i\}$ in stroboscopic sections. Thus, the SSF method can be used. In this section, SSF method of resonant circle in discrete maps [24] is detailed. Rewriting the $1/N$ -period stroboscopic map (13) as:

$$x_{k+1} = g(x_k) + \eta\sigma\zeta_k \tag{15}$$

where:

$$g(x_k) = \exp(J_k\Delta t)x_k \tag{16}$$

$$\eta = \sqrt{\Delta t}\epsilon \tag{17}$$

$$\zeta_k = \Delta w_k / \sqrt{\Delta t} \tag{18}$$

while σ has the same meaning as in Equation (15), ζ_k is n -dimensional Gaussian white noise which satisfies:

$$E[\zeta_t] = 0 \quad E[\zeta_t \zeta_t^T] = I \tag{19}$$

where E is expectation operation, and I is the unit matrix. Equation (13) is rewritten in a simpler form for convenience:

$$x_{k+1} = g_k + \eta \sigma \zeta_k \tag{20}$$

Suppose a quasi-periodic closed curve has been approximated by a period- k one in a one-period stroboscopic map. Thus, in $1/N$ -period stroboscopic map (Equation (20)), all circles $\{\Gamma_i\}$ are periodic- kN , and all points in them are considered to be periodic- kN . For convenience, the range of phase θ is extended from $[\theta_0, \theta_0 + 2\pi]$ to $[\theta_0, \theta_0 + 2k\pi]$, therefore, the number of circles and stroboscopic sections are also extended to kN . However, note that circle $\{\Gamma_i\}$ and $\{\Gamma_{i+\alpha N}\}$ are the same, as are $\{\Sigma_i\}$ and $\{\Sigma_{i+\alpha N}\}$, where $\alpha = 1, 2, \dots, k$.

Consider the periodic $-kN$ points are $\{x_{\Gamma_i}\}$ ($i = 1, 2, \dots, kN$), each x_{Γ_i} belongs to a circle Γ_i in stroboscopic section Σ_i . If a point x_{Γ_i} deviates as:

$$x'_{\Gamma_i} = x_{\Gamma_i} + \eta v_i \tag{21}$$

where v_i is a vector orthogonal to circle Γ_i at point x_{Γ_i} with random length. For small values of η , the evolution of v_i satisfies the linear iterative relation:

$$v_{i+1} = P_{i+1}(G_i v_i + \sigma \zeta_i) \tag{22}$$

where:

$$G_i = \exp(J_i \Delta t) \tag{23}$$

is the Jacobian matrix at x_{Γ_i} . P_{i+1} is the projection matrix onto the hyperplane which is orthogonal to circle Γ_{i+1} at $x_{\Gamma_{i+1}}$. Since ζ_i is weak and Gaussian, the distribution of v_i is considered to be Gaussian, approximately, and its first two order moments follow the iterative relations:

$$\begin{aligned} m_{i+1} &= P_{i+1} G_i m_i \\ M_{i+1} &= P_{i+1} (G_i M_i G_i^T + \sigma \sigma^T) P_{i+1} \end{aligned} \tag{24}$$

Combining Equation (24) with the periodic condition, the SSF of any periodic point on any circle can be calculated. Pick a point arbitrarily in the circle Γ_1 as x_{Γ_1} , it can be proved that the mean of v_1 is zero. Applying the second formula of Equation (24) kN times, and using the periodic condition $M_{kN+1} = M_1$, it can be deduced that the covariance matrix M_1 follows the algebraic equation:

$$M_1 = P_1 (\Phi_1 M_1 \Phi_1^T + Q_1) P_1 \tag{25}$$

where:

$$\Phi_1 = G_{kN} P_{kN} G_{kN-1} P_{kN-1} \cdots F_2 P_2 F_1 \tag{26}$$

Matrix Q_1 can be obtained recurrently:

$$\begin{aligned} Q_1^{(0)} &= 0 \\ Q_1^{(i)} &= P_{i+1} (G_i Q_1^{(i-1)} G_i^T + \sigma \sigma^T) P_{i+1} \quad (i = 1, \dots, kN - 1) \\ Q_1^{(kN)} &= G_i Q_1^{(kN-1)} G_i^T + \sigma \sigma^T \end{aligned} \tag{27}$$

Through the matrix algebraic equation (Equation (25)), M_1 can be calculated directly. Matrix M_1 is named the stochastic sensitivity function (SSF) of x_{Γ_1} because it represents the covariance of out-of-attractor distribution of stochastic attractor at x_{Γ_1} with unity noise intensity.

Based on the recurrence relation (25), M_i ($i = 2, \dots, kN$) can be calculated and the dispersion character of any circle can be quantified. If the circle under analysis is Γ_m , the periodic points on it are $x_{\Gamma_m}, x_{\Gamma(m+N)}, x_{\Gamma(m+2N)}, \dots, x_{\Gamma(m+(k-1)N)}$. Through calculating SSF of these points, the sensitivity of the circle can be approximately depicted.

When the stroboscopic map is planar, every circle is 2D and the SSF can be decomposed as:

$$M_i = \mu_i p_i p_i^T \tag{28}$$

where p_i is normalized vector of v_i . Scalar μ_i quantifies the out-of-circle variance at point x_{Γ_i} with unity noise intensity, which has an explicit form [24]:

$$\mu_i = \frac{p_i^T Q_i p_i}{1 - (p_i^T \Phi_i p_i)^2} \tag{29}$$

Therefore, SSF of 2D circles degenerates into a scalar μ_i , which is the function of point x_{Γ_i} , and the out-of-circle variance of the distribution at point x_{Γ_i} is $\eta^2 \mu_i$. The out-of-circle 1D distribution in a point x is thus given by:

$$\rho_{out}(x) \approx \frac{1}{\eta \sqrt{2\pi \mu(x^*)}} \exp \left\{ -\frac{z(x)^2}{2\eta^2 \mu(x^*)} \right\} \tag{30}$$

4. Procedure of Construct PDF of Stochastic Quasi-Periodic Attractors

From above sections, the procedure to construct approximate expression of the PDF of quasi-periodic torus in a given stroboscopic section is summarized as:

(1) Determine the number N of $1/N$ stroboscopic map and the closed curve to be studied (i of Γ_i , $i=1, 2, \dots, N$). Without loss of generality, suppose the studied circle is Γ_m .

(2) Replace the quasi-periodic circle by an approximate periodic- k one using periodic approximation method. Extend the number of stroboscopic section from N to kN and the scope of indice i is also extended to $[1, kN]$. Thus, the circle is discretized into k points $\{x_{\Gamma_i}\}$, $i = m, m + N, \dots, m + kN$.

(3) Calculate the in-attractor PDF of discretized Γ_m numerically, say, PDF at points $\{x_{\Gamma_i}\}$, $i = m, m + N, \dots, m + kN$. To do this, divide Γ_m into k tiny sections each contains only one point x_{Γ_i} , $i = m, m + N, \dots, m+kN$. Generate a large number of points in this circle to compute the probability to visit every section, and the in-attractor PDF at point x_{Γ_i} is approximated as:

$$\rho_\tau(x_{\Gamma_i}) \approx \frac{P[\Delta s(x_{\Gamma_i})]}{\Delta s(x_{\Gamma_i})} \tag{31}$$

where $P[\Delta s(x_{\Gamma_i})]$ is the probability of the section which contains x_{Γ_i} and $\Delta s(x_{\Gamma_i})$ is the length of it.

(4) Calculate SSF at points $\{x_{\Gamma_i}\}$ using Formula (24)–(27), $i=m, m + N, \dots, m + kN$. Using SSF, confidence intervals ($n = 2$) or confidence ellipses (for $n > 2$) at points $\{x_{\Gamma_i}\}$ can be drawn. Increase N and repeat (1)–(4) until the result converges.

(5) PDF of the studied circle Γ_m can be expressed utilizing formula:

$$\rho(x) \approx \frac{\rho_\tau(x)}{(2\pi)^{\frac{n-1}{2}} |M|^{\frac{1}{2}}} \exp \left\{ -\frac{1}{2} z(x)^T M^{-1} z(x) \right\} \tag{32}$$

or

$$\rho(x) \approx \frac{\rho_\tau(x)}{\eta \sqrt{2\pi \mu(x^*)}} \exp \left\{ -\frac{z(x)^2}{2\eta^2 \mu(x^*)} \right\} \tag{33}$$

for planar circles.

In order to visualize the PDF of the studied circle, the out-of-circle distributions at chosen points on the circle can be plotted within confidence intervals ($n = 2$) or confidence ellipses (for $n > 2$) at given confidence probability. Because the PDF is difficult to visualize when $n > 2$, only $n=2$ cases are taken as examples in this article. PDF or confidence intervals of all the circles $\{\Gamma_i\}$ ($i = 1, 2, \dots, N$) in stroboscopic sections can be drawn to get a global view of the stochastic torus attractor.

5. Examples

The first example is the forced van der Pol oscillator:

$$\begin{aligned}\dot{x} &= y \\ \dot{y} &= -x + \delta y(1 - x^2) + F \cos \omega t + \varepsilon \zeta(t)\end{aligned}\quad (34)$$

where ζ is Gaussian white noise and ε is its intensity. The values of parameters are: $\delta = 1$, $F = 1$, $\omega = 2$, and $\varepsilon = 0.15$. The response of this system is quasi-periodic.

This quasi-periodic attractor is approximated by a periodic-593 attractor (attractor with the period which is 593 times that of the forcing period). The time step of integration is finally determined as $1/500$, so $N = 500$. In Figure 8 three-sigma confidence intervals and the stochastic attractor obtained by the Monte Carlo method in stroboscopic section Σ_1 ($\theta = 2k\pi$, $k = 0, 1, \dots$) is shown. It is calculated that 98.6% of the points are in these intervals, which is very close to 99.73% (three-sigma). To obtain a global and clear view, three-sigma confidence intervals and stochastic attractors in 10 different stroboscopic sections are depicted in Figure 9. It is shown that there is no severe variance of the dispersion of the stochastic closed curves in different stroboscopic sections.

Combining with the in-attractor density, the 2D PDF of stochastic attractors in stroboscopic sections can be obtained. Figure 10a illustrates the 2D PDF of stochastic attractor in stroboscopic section Σ_1 which is drawn within the three-sigma intervals of out-of-attractor Gaussian distributions. The Monte Carlo method is also used to get this PDF (1000×1000 grids and 10^7 points), which is shown in Figure 10b. We can see that the shapes of PDF in Figure 10a,b are almost the same, but the computing time of the proposed method is only 95.78 s, while the Monte Carlo method is 150,732 s.

The second example is the forced Brusselator:

$$\begin{aligned}\dot{x} &= a - (b + 1)x + x^2y + F \cos \omega t + \varepsilon \zeta(t) \\ \dot{y} &= bx - x^2y\end{aligned}\quad (35)$$

where ζ is Gaussian white noise and ε is its intensity. In [20] the disturbed Brusselator was also studied, but the periodic force is tackled as a weak disturbance; thus, the combined action of periodic and random excitation were not studied. In this paper, the parameters of Equation (35) are: $a = 1$, $b = 2.2$, $F = 0.1$, and $\varepsilon = 0.005$. The intensity of noise is chosen as 0.005 because when noise is larger, some out-of-attractor distributions will intersect each other obviously and this means the proposed method no longer works well.

When the forcing frequency $\omega = 2$, this system possesses a quasi-periodic torus attractor. This quasi-periodic attractor is approximated by a periodic-777 attractor. In order to build a $1/N$ -periodic stroboscopic map, set $N = 500$. Three-sigma confidence intervals and the stochastic attractor obtained by the Monte Carlo simulation in stroboscopic section Σ_1 are depicted in Figure 11, and 97.4% of the points are in the intervals. Three-sigma confidence intervals and stochastic attractors in 10 different stroboscopic sections are drawn in Figure 12. It can be seen that there is also no obvious change of the dispersion character of the closed curves in different stroboscopic sections. The PDF of the stochastic attractor in stroboscopic section Σ_1 is drawn in Figure 13a using the proposed method. Compared with the result obtained by the Monte Carlo method (1000×1000 grids and 10^7 points, Figure 13b), it can be seen that the proposed method gives a simple and accurate illustration of the PDF in the forced Brusselator. In this example, the computing time of the proposed method is 102 s while the Monte Carlo method is 154,523 s.

In order to show the limitation of the proposed method, the noise intensity of the Brusselator is increased into 0.05. The results are illustrated in Figure 14. The root mean square (RMS) errors between the proposed method and the Monte Carlo method are calculated for $\epsilon = 0.005$ and $\epsilon = 0.05$, which are listed in Table 1. It can be seen from Figure 14 that the value of the PDF using the proposed method (Figure 14a) is not consistent with the Monte Carlo simulation result (Figure 14b). From Table 1 it is shown that the RMS error, when $\epsilon = 0.05$, is 23.67%, which is much larger than when $\epsilon = 0.005$ (7.57%). The reason is that the Gaussian distributions of some parts intersect with each other heavily (Figure 14c) so Equation (1) does not work well.

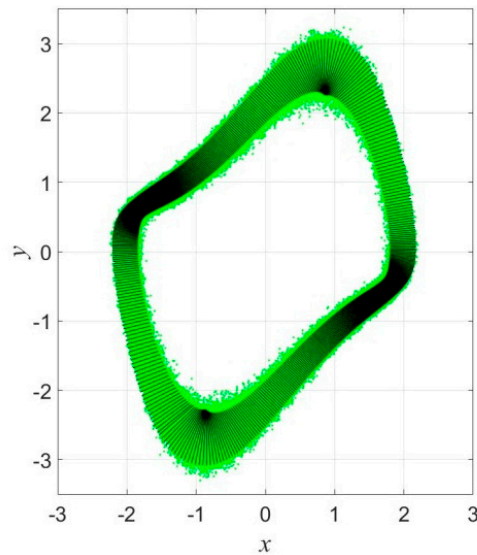


Figure 8. Three-sigma confidence intervals and the stochastic attractor of the forced van der Pol oscillator in stroboscopic section Σ_1 .

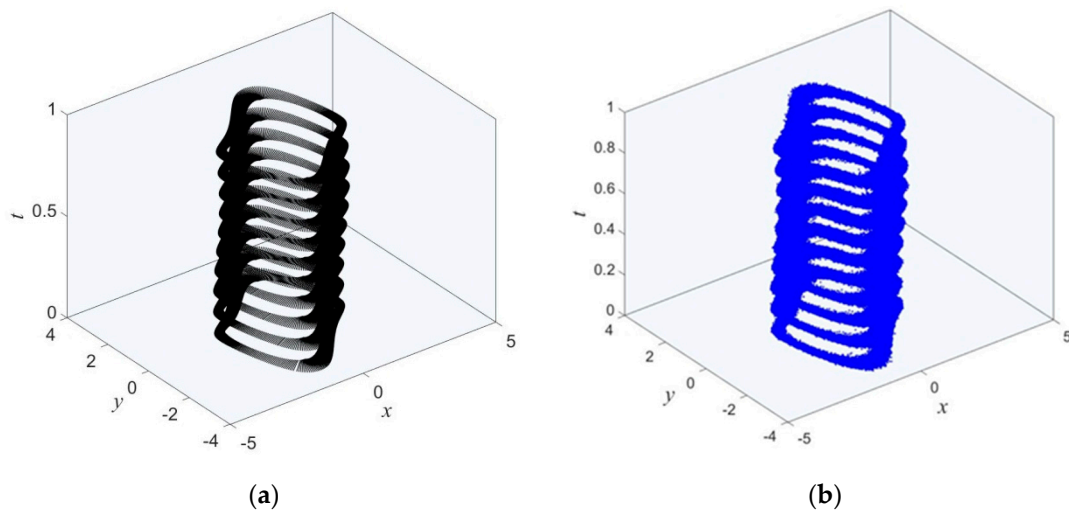
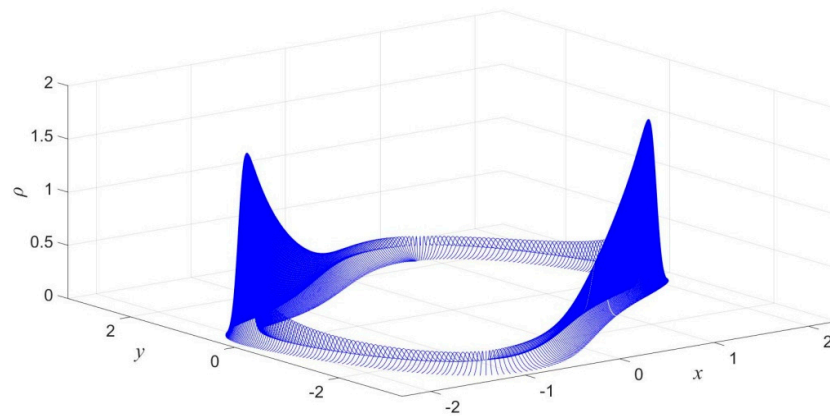
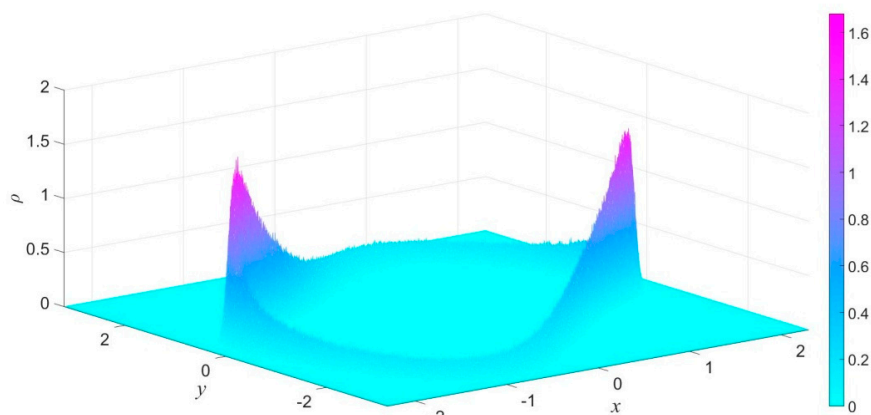


Figure 9. Plots of (a) three-sigma confidence intervals; and (b) the stochastic attractor in 10 different stroboscopic sections of the forced van der Pol oscillator.



(a)



(b)

Figure 10. The PDF of the stochastic attractor of the forced van der Pol oscillator in stroboscopic section Σ_1 (a) obtained by the proposed method; and (b) obtained by the Monte Carlo method.

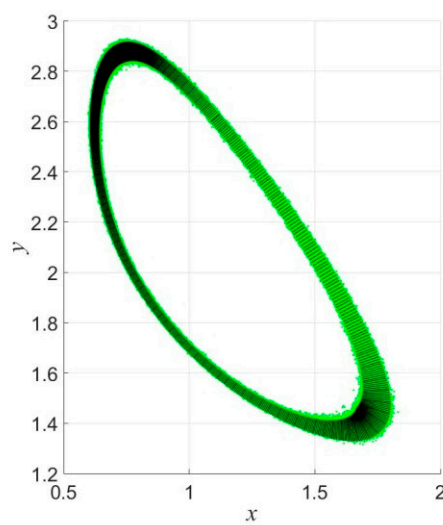


Figure 11. Three-sigma confidence intervals and stochastic attractor of the forced Brusselator in stroboscopic section Σ_1 .

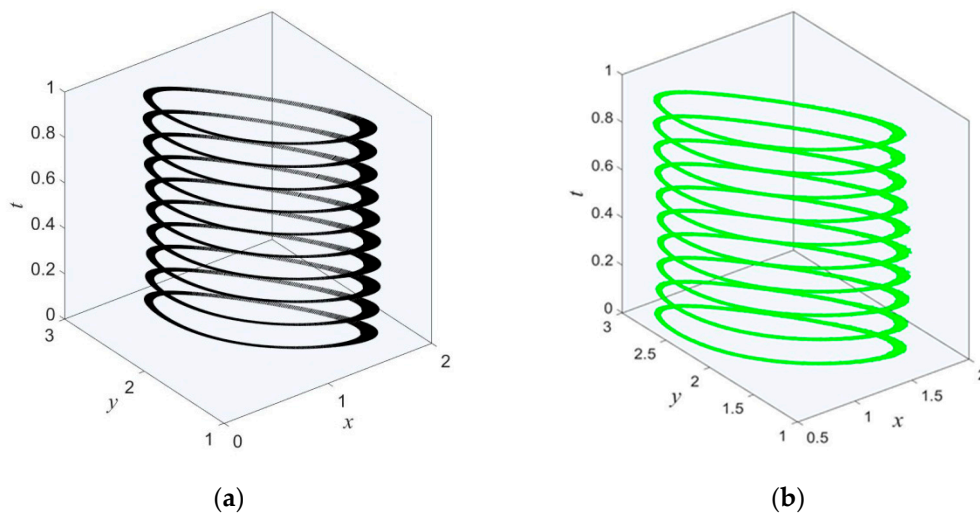


Figure 12. Plots of (a) three-sigma confidence intervals; and (b) the stochastic attractor in 10 different stroboscopic sections of the forced Brusselator.

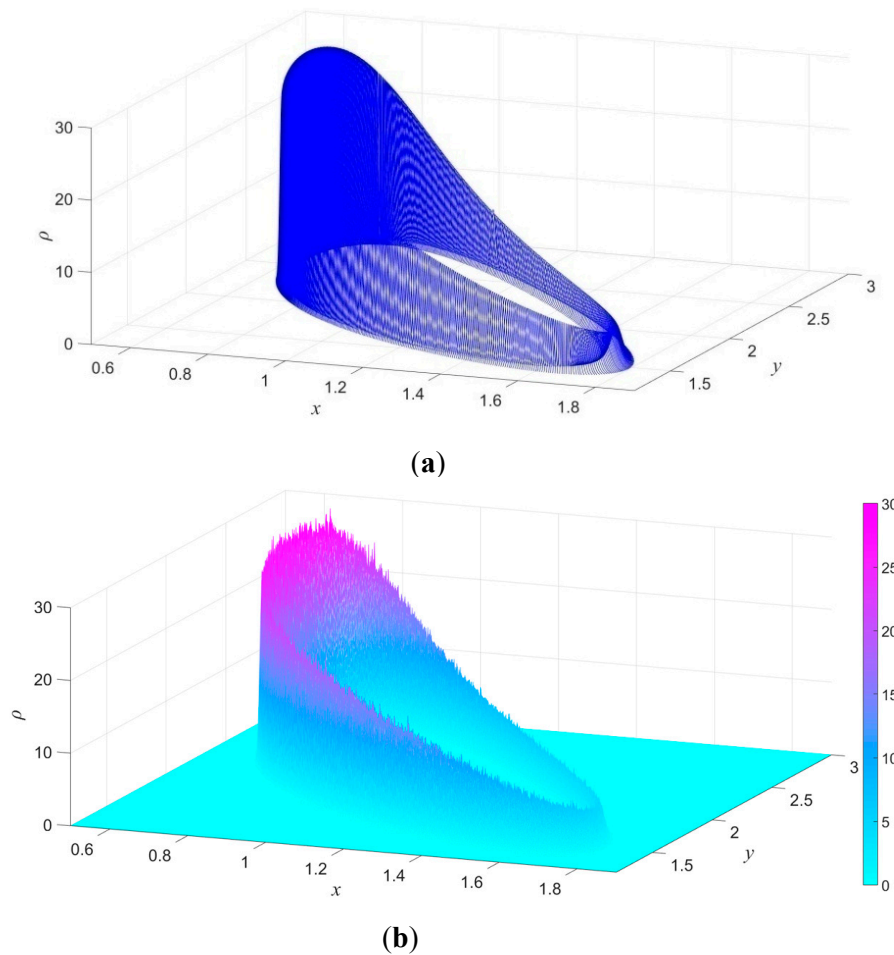


Figure 13. The PDF of the stochastic attractor of the forced Brusselator in stroboscopic section Σ_1 when $\varepsilon = 0.005$ (a) obtained by the proposed method; and (b) obtained by the Monte Carlo method.

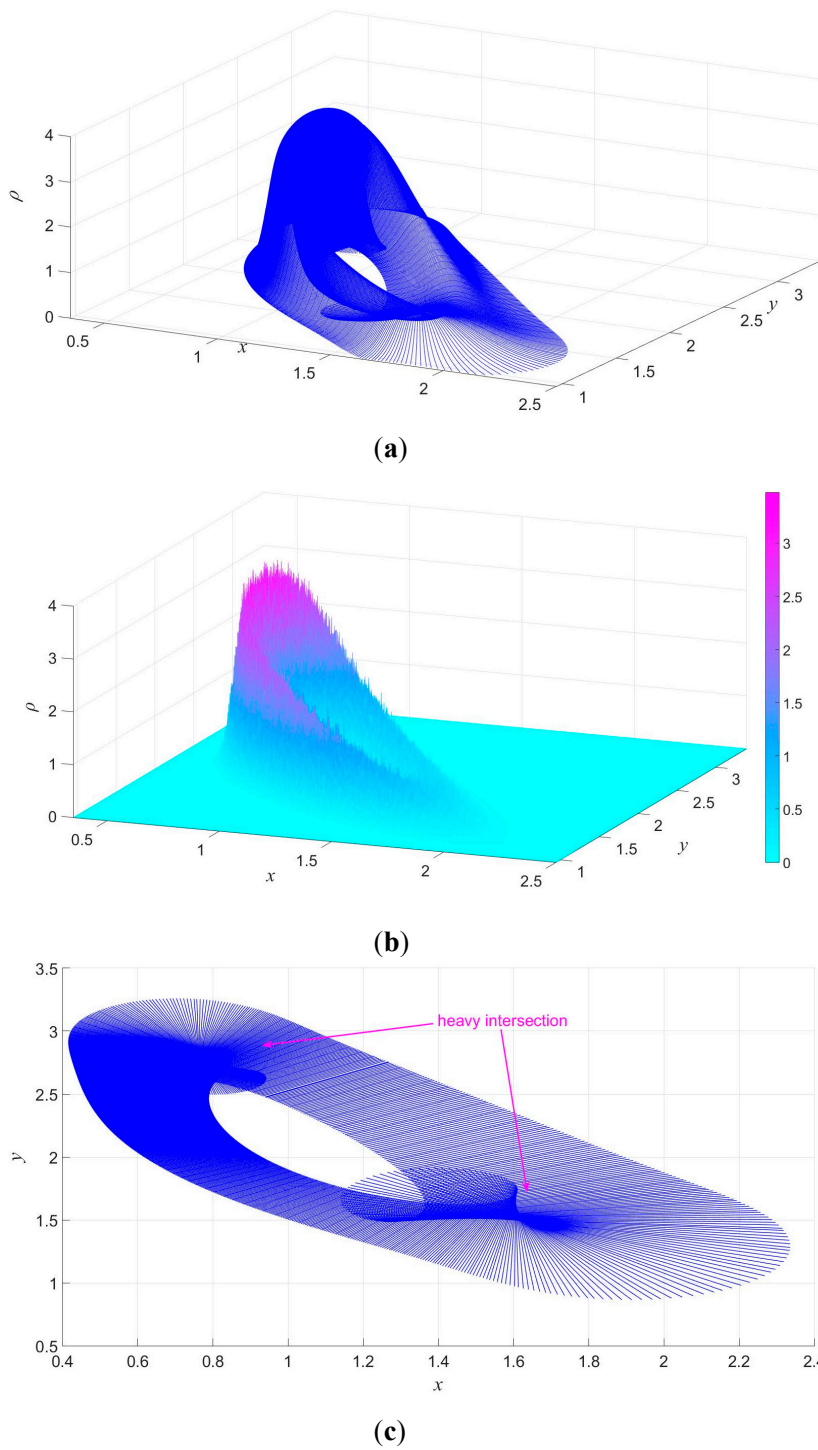


Figure 14. The PDF of the stochastic attractor of the forced Brusselator in stroboscopic section Σ_1 when $\varepsilon = 0.05$ (a) obtained by the proposed method; (b) obtained by the Monte Carlo method; and (c) projection (a) on the xy -plane.

Table 1. Comparison of RMS errors of the Brusselator PDF under two different noise intensities.

Noise Intensity	RMS Error
0.005	7.57%
0.05	23.67%

6. Conclusions

A semi-analytical method to obtain the PDF of quasi-periodic oscillations in non-equilibrium systems under both periodic and weak fluctuation excitations is developed. The $1/N$ -stroboscopic map is introduced to discretize the quasi-periodic torus into closed circles. To obtain the PDF of these stochastic closed circles, the high-dimensional PDF of the stochastic closed circle is decomposed into two low-dimensional distributions, in-attractor PDF and out-of-attractor PDF. The former can be obtained numerically, while the latter is determined by extending the stochastic sensitivity function method through approximating the quasi-periodic attractor as a periodic one. A forced van der Pol oscillator and Brusselator are taken as examples to illustrate the effectiveness of the proposed method. We hope that the method proposed in this work can be extended to solve more complex stochastic nonlinear oscillations in engineering systems.

Acknowledgments: This work is supported by the National Natural Science Foundation of China (11502183 and 11332008), the Natural Science Foundation of Shaanxi Province (2016JM1021), the Postdoctoral Science Foundation of China (2016M592750), and the Fundamental Research Funds for the Central Universities of China (JB150416).

Author Contributions: Jun Jiang proposed the idea; Kongming Guo performed the studies and wrote the paper; and Yalan Xu designed and performed the Monte Carlo simulations.

Conflicts of Interest: The authors declare no conflict of interest.

References

- Ross, J.; Villaverde, A.F. Thermodynamics and fluctuations far from equilibrium. *Entropy* **2010**, *12*, 2199–2243. [[CrossRef](#)]
- Nicolis, C. Stochastic resonance in multistable systems: The role of dimensionality. *Phys. Rev. E* **2012**, *86*, 011133. [[CrossRef](#)]
- Nicolis, G.; Nicolis, C. Stochastic resonance, self-organization and information dynamics in multistable Systems. *Entropy* **2016**, *18*, 172. [[CrossRef](#)]
- Sakaguchi, H. Noise-induced synchronization for phase turbulence. *Phys. Lett. A* **2003**, *318*, 553–557. [[CrossRef](#)]
- Jia, Y.B.; Gu, H.G. Transition from double coherence resonances to single coherence resonance in a neuronal network with phase noise. *Chaos* **2015**, *25*, 123124. [[CrossRef](#)]
- Xu, Y.; Feng, J.; Li, J.J.; Zhang, H.Q. Lévy noise induced switch in the gene transcriptional regulatory system. *Chaos* **2013**, *23*, 013110. [[CrossRef](#)]
- Schindler, M.; Talkner, P.; Hänggi, P. Escape rates in periodically driven Markov processes. *Phys. A Stat. Mech. Appl.* **2005**, *351*, 40–50. [[CrossRef](#)]
- Li, Z.; Jiang, J.; Hong, L. Transient behaviors in noise-induced bifurcations captured by generalized cell mapping method with an evolving probabilistic vector. *Int. J. Bifurc. Chaos* **2015**, *25*, 1550109. [[CrossRef](#)]
- Bashkirtseva, I.; Ryashko, L. Stochastic sensitivity analysis of the attractors for the randomly forced Ricker model with delay. *Phys. Lett. A* **2014**, *378*, 3600–3606. [[CrossRef](#)]
- Billings, L.; Schwartz, I.B. Identifying almost invariant sets in stochastic dynamical systems. *Chaos* **2008**, *18*, 023122. [[CrossRef](#)]
- Lucia, U.; Gervino, G. Fokker-Planck equation and thermodynamic system analysis. *Entropy* **2015**, *17*, 763–771. [[CrossRef](#)]
- Chen, L.C.; Sun, J.Q. The closed-form solution of the reduced Fokker-Planck-Kolmogorov equation for nonlinear systems. *Commun. Nonlinear Sci. Numer. Simul.* **2016**, *41*, 1–10. [[CrossRef](#)]
- Wu, Y.; Zhu, W.Q. Stationary response of multi-degree-of-freedom vibro-impact systems to Poisson white noises. *Phys. Lett. A* **2008**, *372*, 623–630. [[CrossRef](#)]
- Kougioumtzoglou, I.A.; Spanos, P.D. An analytical Wiener path integral technique for non-stationary response determination of nonlinear oscillators. *Probab. Eng. Mech.* **2012**, *28*, 125–131. [[CrossRef](#)]
- Kumar, M.; Chakravorty, S.; Singla, P.; Junkins, J.L. The partition of unity finite element approach with hp-refinement for the stationary Fokker-Planck equation. *J. Sound Vib.* **2009**, *327*, 144–162. [[CrossRef](#)]
- Billings, L.; Bollt, E.M.; Schwartz, I.B. Phase-space transport of stochastic chaos in population dynamics of virus spread. *Phys. Rev. Lett.* **2002**, *88*, 234101. [[CrossRef](#)]

17. Tél, T.; Lai, Y.C. Quasipotential approach to critical scaling in noise-induced chaos. *Phys. Rev. E* **2010**, *81*, 056208. [[CrossRef](#)]
18. Ge, H.; Qian, H. Landscapes of non-gradient dynamics without detailed balance: Stable limit cycles and multiple attractors. *Chaos* **2012**, *22*, 023140. [[CrossRef](#)]
19. Kwon, C.; Ao, P. Nonequilibrium steady state of a stochastic system driven by a nonlinear drift force. *Phys. Rev. E* **2011**, *84*, 061106. [[CrossRef](#)]
20. Bashkirtseva, I.A.; Ryashko, L.B. Sensitivity analysis of the stochastically and periodically forced Brusselator. *Phys. A Stat. Mech. Appl.* **2000**, *278*, 126–139. [[CrossRef](#)]
21. Skurativskyi, S.I.; Skurativska, I.A. Dynamics of traveling waves in fluctuating nonlocal media. *Commun. Nonlinear Sci. Numer. Simul.* **2017**, *49*, 9–16.
22. Guo, K.; Jiang, J.; Xu, Y. Semi-analytical expression of stochastic closed curve attractors in nonlinear dynamical systems under weak noise. *Commun. Nonlinear Sci. Numer. Simul.* **2016**, *38*, 91–101. [[CrossRef](#)]
23. Bashkirtseva, I.; Ryashko, L. Sensitivity analysis of stochastically forced quasiperiodic self-oscillations. *Electron. J. Diff. Eq.* **2016**, *240*, 1–12.
24. Bashkirtseva, I.; Ryashko, L. Stochastic sensitivity of the closed invariant curves for discrete-time systems. *Phys. A* **2014**, *410*, 236–243. [[CrossRef](#)]
25. Guo, K.M.; Jiang, J. Stochastic sensitivity analysis of periodic attractors in non-autonomous nonlinear dynamical systems based on stroboscopic map. *Phys. Lett. A* **2014**, *378*, 2518–2523. [[CrossRef](#)]
26. Aronson, D.G.; Chory, M.A.; Hall, G.R.; McGehee, R.P. Bifurcations from an invariant circle for two-parameter families of maps of the plane: a computer-assisted study. *Commun. Math. Phys.* **1982**, *83*, 303–354. [[CrossRef](#)]



© 2017 by the authors. Licensee MDPI, Basel, Switzerland. This article is an open access article distributed under the terms and conditions of the Creative Commons Attribution (CC BY) license (<http://creativecommons.org/licenses/by/4.0/>).